Brain Responses to Success and Failure: Direct Recordings from Human Cerebral Cortex

Julien Jung,[1,2]* Karim Jerbi,[1,3] Tomas Ossandon,[1] Philippe Ryvlin,[1,2] Jean Isnard,[1,4] Olivier Bertrand,[1] Marc Guénot,[4,5] François Mauguière,[2,4] and Jean-Philippe Lachaux[1]

[1]*Brain Dynamics and Cognition, INSERM U821, Lyon, France*
[2]*Department of Epileptology and Functional Neurology, Neurological Hospital, Lyon, France*
[3]*Physiology of Perception and Action Laboratory, CNRS, UMR 7152, Collège de France, Paris, France*
[4]*Sensory Integration of Pain, INSERM U879, Lyon, France*
[5]*Department of Neurosurgery, Neurological Hospital, Lyon, France*

Abstract: Evaluating the outcome of our own actions is a fundamental process by which we adapt our behavior in our interaction with the external world. fMRI and electrophysiological studies in monkeys have found feedback-specific responses in several brain regions, unveiling facets of a large-scale network predominantly distributed in the frontal lobes. However, a consensus has yet to be reached regarding the exact contribution of each region. The present study benefited from intracerebral EEG recordings in epileptic patients to record directly the neural activity in each of those frontal structures in response to positive and negative feedback. Both types of feedback induced a sequence of high-frequency responses (>40 Hz) in a widespread network involving medial frontal cortex, dorsolateral prefrontal cortex (DLPFC), orbitofrontal cortex (OFC), and insular cortex. The pre-supplementary motor area (pre-SMA), DLPFC, and lateral OFC showed higher activation in response to negative feedback, while medial OFC and dorsal anterior cingulate cortex (dACC) were more responsive to positive feedback. Responses in the medial prefrontal cortex (pre-SMA and dACC) were sustained (lasting more than 1,000 ms), while responses in the DLPFC, insula, and the OFC were short lasting (less than 800 ms). Taken together, our findings show that evaluating the outcome of our actions triggers γ-range activity modulations in several frontal and insular regions. Moreover, we found that the timing and amplitude of those γ-band responses reveal fine-scale dissociations between the neural dynamics of positive versus negative feedback processing. *Hum Brain Mapp 31:1217–1232, 2010.* © 2010 Wiley-Liss, Inc.

Key words: γ-band oscillations; intracranial EEG; performance monitoring; epilepsy; executive functions

INTRODUCTION

"... We regret to inform you that we cannot recommend your manuscript for publication ...". Whether you are a researcher reading such a notification or an NBA player witnessing the fraction of a second your ball bounces backwards off the rim of the basketball, your interaction with the outside world is a constant source of feedback evaluating your actions on multiple time scales.

Additional Supporting Information may be found in the online version of this article.

Contract grant sponsor: NeuroProbes (EU Research Program); Contract grant number: FP6-IST 027017 (to KJ); Contract grant sponsor: NeuroBotics (EU Research Program); Contract grant number: FET FP6-IST-001917 (to KJ).

*Correspondence to: Julien Jung, MD, PhD, Brain Dynamics and Cognition, INSERM - Unité 821, Centre Hospitalier Le Vinatier, Bâtiment 452, 95 Boulevard Pinel, 69500 Bron, France. E-mail: julien.jung@inserm.fr

Received for publication 9 January 2009; Revised 28 July 2009; Accepted 28 September 2009

DOI: 10.1002/hbm.20930

Published online 29 January 2010 in Wiley InterScience (www.interscience.wiley.com).

Our ability to use this feedback to adapt our behavior is critical in all aspects of our life. Lesion studies and the effect of pathologies have shown that this capacity depends critically on the frontal cortex (Alexander et al., 2007; Polli et al., 2008; Thakkar et al., 2008)

In the last 15 years, electrophysiological and neuroimaging studies have provided a more detailed understanding of how the frontal cortex respond to negative (or positive) feedback. Human event-related potential (ERP) studies have shown that negative feedback signals generate an enhanced negative component, as compared to positive feedback, peaking over frontocentral electrodes with a latency of 300 ms (Miltner et al., 1997) and referred to as "feedback-related negativity (FRN)" [but see Holroyd et al. (2008) for alternative interpretation]. Several EEG studies using Source localization have identified the anterior cingulate cortex (dACC) as the most likely generator of the FRN (Gehring and Willoughby, 2002; Luu et al., 2003; Miltner et al., 1997; Ruchsow et al., 2002). In accordance, several fMRI studies have shown increased dACC activation when subjects receive negative feedback (Holroyd et al., 2004; Ullsperger and von Cramon, 2003) despite some discrepancies across studies (Cools et al., 2002; Nieuwenhuis et al., 2005; van Veen et al., 2004).

Moreover, fMRI studies have shown that feedback evaluation activates not only the dACC but also several brain regions including medial prefrontal cortex (Ullsperger and von Cramon, 2003), dorsolateral prefrontal cortex (DLPFC) (Zanolie et al., 2008), orbitofrontal cortex (OFC) (Walton et al., 2004; Zanolie et al., 2008), and insula (Zanolie et al., 2008), depending on the studies.

Single-cell recordings in nonhuman primates indicate that feedback evaluation leads to modulations of neuronal firing in several structures within that frontal network including the dACC (Ito et al., 2003; Michelet et al., 2007; Quilodran et al., 2008), the DLPFC (Matsumoto et al., 2007), and the OFC (Wallis, 2007).

Clearly, feedback stimuli elicit distributed neural responses in a brain network that seems to be more complex than what was initially suggested by source localization of the FRN in human ERP studies. fMRI studies, backed up by monkey electrophysiology, have shown that this network might involve not only the medial frontal cortex including the dACC and pre-supplementary motor area (pre-SMA), but also the DLPFC, the OFC, and the insula. However, to our knowledge, all previous studies have reported only piecewise activations of that network, the exact extent of which remains undetermined. Moreover, the timing of activation of those structures during feedback evaluation remains largely unknown.

The objective of the present study was to clarify the neural bases of feedback evaluation by recording the response to feedback stimuli in all previous structures in humans, with direct neural recordings. Direct electrophysiological recordings can be achieved in epileptic patients with intracerebral electrodes implanted for therapeutic purposes (Lachaux et al., 2003), to record neural activity with a spatial resolution comparable to fMRI, and millisecond temporal resolution. In particular, stereo-encephalography (SEEG), using linear-electrode areas recording from both lateral and mesial structures, from both gyri and sulci, provides a unique opportunity to investigate all regions assumed to participate in feedback monitoring, such as the DLPFC and the dACC.

The present work was triggered by a recent series of intracranial EEG studies showing that broadband energy increase of neural signals (50–150 Hz, the so-called γ-band) constitutes a precise marker identifying neural recruitment during cognitive processing (Jensen et al., 2007; Jerbi et al., 2009; Lachaux et al., 2003). Such γ-band responses (GBRs) have been used to map the large-scale cortical networks underlying several major cognitive functions, including language processing (Jung et al., 2008; Mainy et al., 2008), memory (Mainy et al., 2007), attention (Jensen et al., 2007), and top–down processes (Engel et al., 2001; Kahana, 2006). Those results are in line with a possible role of γ-band neural synchronization in local and large-scale neural communication (Fries et al., 2007; Lee, 2003; Singer, 1999; Varela et al., 2001). Further, recent studies combining electrophysiological and BOLD measures using fMRI have found a strong correlation between GBRs and the BOLD signal (Lachaux et al., 2007; Logothetis et al., 2001; Mukamel et al., 2005). Based on those results, we predicted that feedback stimuli would trigger GBRs in several brain structures activated during fMRI studies, including the medial frontal wall, the DLPFC, the OFC, and the insula. Moreover, we anticipated that possible differences in timing would help delineate functional dissociations within that network.

MATERIALS AND METHODS

Participants

Nine subjects (six females and three males, aged 19–56 years, mean = 36 years) participated in this study. They all suffered from drug-resistant partial epilepsy and were candidates for surgery. They had normal or corrected-to-normal vision and were not colorblind. Because the location of the epileptic focus could not be identified using noninvasive methods, the patients underwent intracerebral EEG recordings by means of stereotactically implanted multilead depth electrodes (SEEG) [for a complete description of the rationale of electrode implantation, see Isnard et al. (2000)]. The selection of the sites to implant was made entirely for clinical purposes with no reference to the present experimental protocol. Patients who took part in this study were selected, because their implantation included various regions of the frontal lobe or insular cortex. The activated sites reported in the Results section were always outside of the seizure onset zone of the patients. The patients performed the task 2 days after the implantation of the electrodes. In agreement with French regulations relative to invasive investigations with a direct

TABLE I. Overview of anatomical regions exhibiting significant GBRs induced by feedback stimuli

	Pre-SMA	dACC	DLPFC	Mesial OFC	Lateral OFC	Insula
No. of sites recorded	9	11	15	9	9	10
No. of significant GBRs (% sites)	5 (55)	2 (18)	4 (27)	4 (44)	2 (22)	6 (60)
No. of nonspecific GBRs (% significant GBRs)	0 (0)	0 (0)	1 (25)	0 (0)	0 (0)	0 (0)
No. of positive feedback (% significant GBRs)	0 (0)	2 (100)	0 (0)	4 (100)	0 (0)	1 (17)
No. of negative feedback (% significant GBRs)	5 (100)	0 (0)	3 (75)	0 (0)	2 (100)	5 (83)

Feedback stimuli induced statistically significant GBRs clustered in a well-defined set of anatomical structures across patients. For each cluster, the total number of recording sites and the number and the percentage of sites with significant GBRs is provided. The number and percentage of sites with a feedback preference to error (negative), correct (positive), or nonspecific for each cluster is given.

individual benefit, patients were fully informed about electrode implantation, stereotactic EEG (SEEG), evoked potential recordings, and cortical stimulation procedures used to localize the epileptogenic and eloquent cortical areas, and the patients gave their informed consent.

Electrode Implantation and Coregistration

The electrodes used consisted of one-dimensional arrays implanted orthogonal to the interhemispheric plane using the Talairach's stereotactic grid. Brain activity was recorded in 5–15 contact sites along each electrode. Spacing between consecutive sites was 3.5 mm (center-to-center), which correspond to the estimated spatial resolution of the recordings (Lachaux et al., 2003). The electrodes were left chronically in place for up to 15 days. The electrode positions were reconstructed onto individual MRI through the superposition of the computed tomography scan images showing the electrodes, the angiography, and the patient's structural MRI slices (using the software Activis package, Lyon, France).

To compare electrode position and summarize brain activations across patients, electrode coordinates were also converted from the individual Talairach space to the normalized Talairach space (Talairach and Tournoux, 1988). Coordinates provided in this study are in the normalized Talairach space. In addition, those coordinates were further converted into the Montreal Neurological Institute (MNI) standard brain space for visualization purpose onto 3D renderings of the single-subject MNI brain. Cortical surface segmentations were performed with the BrainVisa package (CEA, France).

Spatial Sampling

Across the nine patients, we recorded from a total of 59 one-dimensional depth electrodes in the frontal and insular cortex (see Supporting Information Fig. 1 showing all recording sites in the frontal lobes). The total number of recording contacts was 917, distributed in both gray and white matter. For clarity, sites found active in the present paradigm were grouped into distinct anatomical clusters (see Tables I and II for a list of those clusters). Because of the interindividual anatomical variability, the cluster definition was not based on proximity in the Talairach space. Rather, sites were pooled into the same cluster if they belonged to the same anatomical structure, defined on the individual MRI by anatomical (gyri and sulci) or functional landmarks well established in the literature [e.g., the distinction between SMA and pre-SMA (Picard and Strick, 1996)].

Experiment

All participants performed two distinct tasks on the same day. The main experiment consisted of a time-estimation task involving performance monitoring (PM) via visual feedback. This experiment was preceded by a simple visual oddball task, which was used as a control condition [control task (CT)].

PM task

We implemented a paradigm very similar to the one used by Miltner et al. (1997) in a seminal EEG study reporting feedback-related potentials. Participants played a classic time-estimation game in which the aim was to press twice on a button with an interval of exactly 1 s (see Fig. 1). Each trial started with the presentation of a white fixation cross at the center of a black screen. After 500 ms, the color of the cross switched to blue to instruct the participant to play (GO signal). When ready, the participant would press the same joystick button twice to produce a 1-s interval. The performance for this trial was defined as the absolute difference between the actual duration of that interval and the target duration (1,000 ms). Three seconds after the second button press, the central fixation cross was replaced with a small square (FEEDBACK signal) the color of which indicated "success" or "failure." A green square indicated that the performance was below the tolerated margin of error (positive feedback), while a red square indicated that the performance was above the margin (negative feedback). Three seconds after the feedback signal, the actual quantitative performance was displayed (e.g. "−236 ms") for 1 s to allow behavioral adjustment in the next trial. Finally, each trial ended with a 1-s display of the overall score obtained by the participant; starting at 0 at the beginning of a block, the score increased by steps of 1 or 2 with each successful trial, depending on

TABLE II. Talairach coordinates for the recording sites exhibiting different GBRs for positive and negative feedback and presented in Figures 3–6

Cluster	Patient no.	Electrode	x (mm)	y (mm)	z (mm)	Side
Pre-SMA	P2	s2	7	2	52	R
	P3	q′2	−9	1	57	L
	P6	s2	8	2	52	R
	P7	s2	6	10	50	R
	P9	s2	11	4	50	R
dACC	P3	w′3	−11	17	32	L
	P6	k3	8	32	25	R
DLPFC	P3	w′10	−37	17	32	L
	P4	f′11	−37	58	13	L
	P7	f′11	−44	32	31	L
OFC	P1	k7	26	54	7	R
	P1	o11	40	40	−3	R
	P2	e7	27	31	7	R
	P3	e′8	−32	40	−7	L
	P3	e′12	−42	40	−7	L
	P5	o6	25	42	−11	R
Insula	P1	i6	34	10	1	R
	P1	p3	30	16	15	R
	P3	p′2	−33	6	16	L
	P3	t′3	−40	−3	0	L
	P5	t2	33	14	−7	R
	P6	n3	54	−15	19	R

Twenty-three sites across the nine patients exhibited GBRs that differed between positive and negative feedback. x, y, and z refer to the Talairach coordinates (not the MNI coordinates) of the sites (in millimeters). The implanted hemisphere for each site is provided (L = left, R = right). These values were converted to MNI coordinates for display onto the MNI single subject MRI.

performance (see paragraph below). The challenge was to reach a total score of 14 in as few trials as possible, at which point the block ended. Each block was ended after a maximum of 20 trials even if the score of 14 had not been reached. According to the patients' verbal reports, using reduction of the duration of the experiment as a reward for good performance proved to be an efficient way of motivating them.

One critical parameter of the task was the margin of error tolerated in each trial. Because we intended to compare neural responses to positive and negative feedback, we designed the experiment to balance the number of wins and losses. For this purpose, the margin was adjusted to performance on a trial-to-trial basis. Margin was initially set to 200 ms, which meant that any interval between 800 and 1,200 ms was evaluated as "correct." The tolerated margin for each new trial was continuously adapted to the performance in all previous trials since the beginning of the experiment: if e_i is the error at trial i (interval between button the two presses minus 1,000 ms), then the margin was the standard deviation of all previous e_i values. A successful trial was then defined by an error less than the standard deviation of all previous trials (score increased by 1). To further increase motivation, the participants were rewarded with an additional point if their error was less than half the tolerated margin (the score increased by 2).

Each participant performed a total of 16 blocks (yielding between 172 and 213 trials) and was told that the aim was to finish the experiment by reaching the target score (14 points) as quickly as possible and that the accuracy of his performance would be rewarded by an increase of the score. The total duration of the experiment varied with participant's performance and ranged between 1 and 1.5 h.

Control task

The CT used the same visual stimuli as those used in the PM task in a neutral context with no feedback value (a detailed description of the CT is given in Supporting Information Procedures).

Participants responded by pressing a joystick button with their right index finger. The experimental procedure took place in patient's hospital room. Stimuli were presented to the participants on a 17″ computer screen at a 56 cm viewing distance using the stimulus software presentation (Neurobehavioral Systems). Square stimuli subtended a horizontal and vertical angle of ∼4°.

Recording and Data Analysis

Intracerebral recordings were conducted using an audio-video-EEG monitoring system (Micromed, Treviso, Italy),

which allowed for simultaneous acquisition of data from upto 128 depth-EEG channels sampled at 512 Hz (0.1–200 Hz bandwidth) during the experimental paradigm. All signals were rereferenced to their nearest neighbor on the same electrode, 3.5 mm away before analysis (bipolar montage). Recording sites showing epileptiform activities were excluded from the analysis, and among the remaining sites, bipolar data were systematically inspected, and any trial showing epileptic spikes in any of those traces was discarded. All signals analyzed in this study were recorded from sites far from the a posteriori revealed seizure focus.

Data Analysis

We analyzed the acquired data in time–frequency (TF) domain to address three specific questions: First, are there any feedback-induced neural power modulations compared to a prestimulus baseline period? Second, are such activations (if any exist) distinguishable from responses elicited by the mere presentation of the same stimuli in the control condition (irrespective of feedback context)? Third, are those neural responses differentially modulated by the valence of the feedback (positive vs. negative)?

For each stimulus category ("positive" or "correct" vs. "negative" or "error"), the data were segmented into windows extending from 3,000 ms before stimulus onset to 3,000 ms after stimulus onset. Next, individual data segments were transformed into TF power representations, following our routine procedure (Jung et al., 2006): for each single trial, bipolar derivations computed between adjacent electrode contacts were analyzed in the TF domain by convolution with complex Gaussian Morlet's wavelet (Tallon-Baudry et al., 1997) thus providing a TF power map $P(t,f) = |w(t,f)*s(t)|^2$, where $w(t,f)$ was for each time t and frequency f; a complex Morlet's wavelet $w(t,f) = A \exp(-t^2/2\sigma_t^2)\exp(2i\pi ft)$, with $A = (\sigma\sqrt{\pi})^{-1/2}$, $\sigma_t = 1/(2\pi\sigma_f)$, and σ_f a function of the frequency f: $\sigma_f = f/7$. The result of this procedure is a TF map for each recording site and for each epoch presenting the signal power as a function of time (from −3,000 to 3,000 ms relative to stimulus onset) and frequency (from 1 to 150 Hz). See Supporting Information Figure 2 for an overview of the TF analysis. Additionally, to determine whether oscillatory responses were phase-locked to the stimulus, we computed TF maps of the phase-locking factor (Tallon-Baudry et al., 1997) and compared the values obtained after the stimulation with the values during the baseline.

The effect of the stimulus on TF power can then be evaluated at each frequency by comparing statistically pre- and post-stimulus power values. This comparison was done with Wilcoxon nonparametric tests that compared across epochs, the total power in a given TF tile, with that of a tile of similar frequency extent, but covering a [−500:0 ms] prestimulus baseline period. For each recording site, we performed 2,280 Wilcoxon tests to cover a set of [100 ms × 4 Hz] TF tiles covering a [−3,000:3,000 ms] × [1:150 Hz] TF domain. Statistical threshold was set to $P < 0.05$, corrected for multiple comparisons across tiles and recording sites with the false discovery rate method (Genovese et al., 2002). This procedure was used to identify sites with significant feedback-related power changes in the PM task and with no significant response to the same stimuli in the CT. In such sites, characterized by responses related and specific to feedback, TF power was compared between positive and negative feedback. This comparison was done on the power measured in a global TF domain covering the significant responses to feedback stimuli. More precisely, for each type of feedback, and for each site, the TF extent of the response could be defined as the collection of all contiguous TF tiles with significantly higher or lower power than baseline (using Wilcoxon test). The global TF domain used for this comparison was the smallest TF domain that covers the TF response to both positive and negative feedbacks. The statistical test used a Mann–Whitney U test to compare across epochs the average power value measured in that TF domain between positive and negative feedbacks. Note that P values were corrected for multiple comparisons with the Bonferroni method.

Note that Figure 2 displays the envelope of γ-band energy in response to feedback signals, averaged across trials and recording sites for each cluster. That is, all epochs recorded within a cluster (and corresponding to different sites and patients) were considered as if recorded from one single recording site in a single patient. Raw signals were band-pass-filtered in ten consecutive frequency bands [from (50–60 Hz) to (140–150 Hz), by steps of 10 Hz], and for each band, the envelope of the band-pass-filtered signal was computed with a Hilbert transform. For each band, this envelope signal was divided by its mean value across the entire recording session and multiplied by 100 so that envelope values are expressed in percent of that mean value. Finally, the envelope signals computed for each of the ten frequency bands were averaged together, to provide one single time-series (the γ-band envelope) for the entire session. By construction, the mean value of that time-series across the recording session is equal to 100. Figure 2 displays the average and standard error of the mean of that γ-band envelope, across trials, expressed in percent of increase or decrease relative to 100. For each type of feedback and each cluster, the mean peak amplitude (±standard error of the mean) and mean peak latency of the GBRs were measured on those γ-band envelopes.

Note that that visualization has the advantage of summarizing the most prominent responses, but does not fully capture the intersubject variability of the responses. It should thus be qualified by results shown at the individual level, shown in the remaining figures.

ERP Analysis

ERPs were measured by averaging data segments across epochs in the time domain. Comparison between ERPs to positive and negative feedback were done with a nonparametric Mann–Whitney U test on consecutive 20 ms

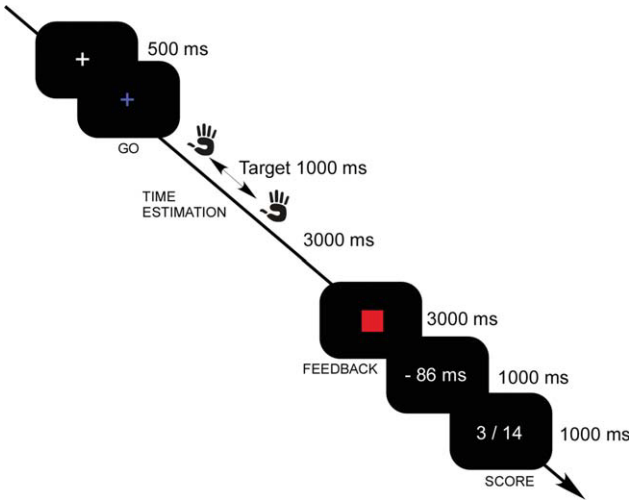

Figure 1.

PM paradigm. Each trial started with the presentation of a white central fixation cross at the center of a black screen. The cross turned blue 500 ms later (GO signal) instructing the participants to generate a 1-s duration via two consecutive joystick button presses. A colored square was displayed as feedback on performance 3,000 ms after the second button press. The square was either green (correct/postive feedback) or red (error/negative feedback) and remained visible for 3,000 ms. This qualitative feedback was then followed by a quantitative feedback (millisecond estimation error, e.g., "−86 ms") presented for 1,000 ms and followed by an overall score update. Task difficulty was adapted on-line to balance the number of positive and negative feedback stimuli (see Materials and Methods). [Color figure can be viewed in the online issue, which is available at www.interscience.wiley.com.]

overlapping windows (1 ms step). All EEG signals were evaluated with the software package for electrophysiological analysis (ELAN-Pack) developed in the INSERM U821 Laboratory and with custom MATLAB (The MathWorks) code.

RESULTS

Behavioral Results

Overall, the intervals measured differed from the intended duration by 265 ms (±191 ms). But since the tolerated error margin was adjusted during the course of the experiment (see Materials and Methods for details), there was no significant difference between the number of correct (87 ± 31) and incorrect trials (89 ± 31) (Mann–Whitney U test, $P > 0.05$). Subject performance improved over time, suggesting that the participants did indeed use the feedback information to adapt their behavior. A statistical analysis showed that estimation errors were larger in the first third of the experiment (first 33% trials) than in the last third (384 > 181 ms, Wilcoxon signed rank test, $P < 0.001$).

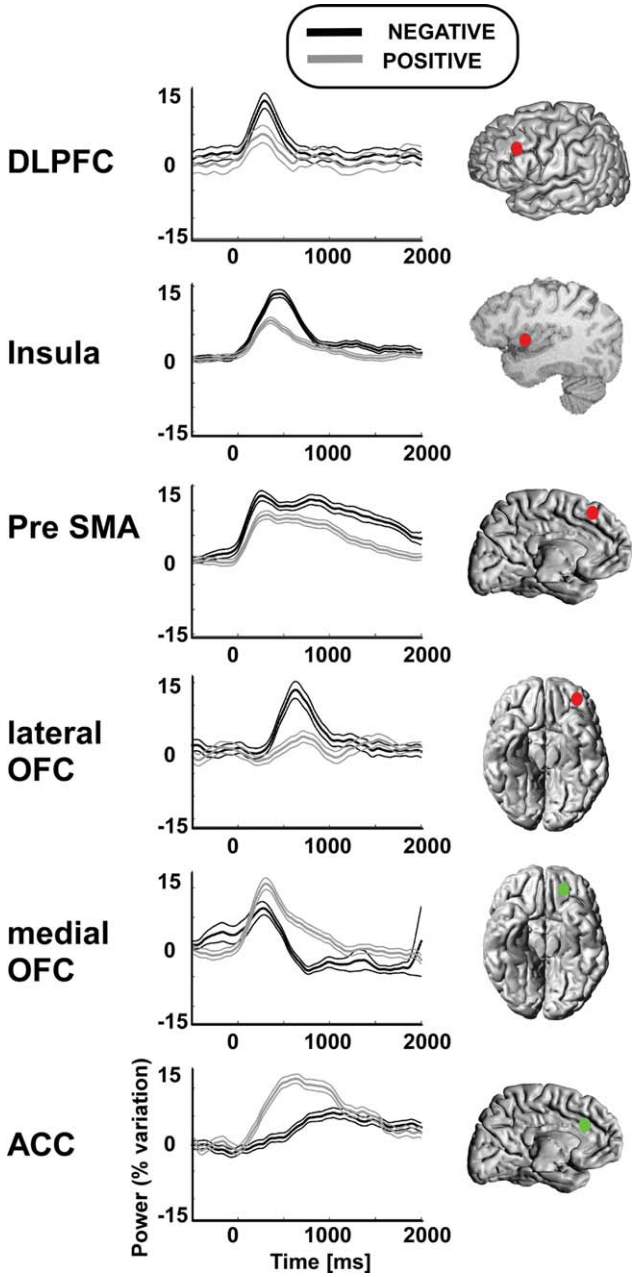

Figure 2.

Overview of the dynamics of the high-frequency responses induced by feedback stimuli. Six anatomical clusters exhibit significant GBRs in response to feedback stimuli. For each cluster, the envelope of GBRs (with standard error of the mean) was averaged across patients and the average response is presented for "error" (i.e., negative feedback, black line) and "correct" (i.e., positive feedback, gray line). Time 0 is the onset of visual feedback. [Color figure can be viewed in the online issue, which is available at www.interscience.wiley.com.]

The Neural Bases of PM: Frontoinsular Neural Network Generating GBRs to Feedback Stimuli

A full-band TF analysis of neural responses to feedback was performed for all recording sites, and it revealed that the most reproducible responses across individuals were in the high-frequency γ-band (>40 Hz) (see however Supporting Information Fig. 3 for examples of TF responses in other frequency bands).

During the PM task, 88 bipolar derivations (out of 917 in nine patients) had a significant energy modulation above 40 Hz after feedback stimuli (Wilcoxon comparison with prestimulus baseline, corrected $P < 0.05$). When several contiguous active bipolar derivations explored the same anatomical structure in the same patient (for example, four sites exploring the dACC), they were further considered as exploring one single site [explaining the total number of active sites (23) shown in Tables I and II].

Those GBRs were induced, and not evoked, by the stimulus; in other words, they were not phase-locked to the stimulus (as indicated by a phase-locking factor analysis).

As responses to feedback in the PM task could theoretically be simply related to visual processing of the stimuli, a CT was performed by all patients. The CT used the same stimuli in a neutral context with no feedback value (a detailed description of the CT is given in Supporting Information Procedures). The CT and the PM task use the same stimuli, but with a different meaning. The comparison between the responses triggered by red/green squares in the PM task and the CT reveals which response components are associated with the particular meaning of those stimuli, as performance feedback. Supporting Information Figure 4 illustrates the striking difference in brain activation induced by meaning alone: as soon as 300 ms after stimulus presentation, the visual stimuli ignite the frontal cortex only in the PM condition, that is, only when they contain meaningful information about feedback. The comparison between the CT and PM task was therefore a way to isolate feedback-specific responses: in the remaining section, any frontal site that also responded to the red/green squares in this neutral control context (example in Supporting Information Fig. 5) was considered nonspecifically feedback-related and was therefore excluded from the analysis and discussions below.

Although the overall spatial coverage of the frontal lobe across the nine patients was extensive, high-frequency responses were found only in spatially restricted anatomical clusters (see Tables I and II for a list of anatomical clusters). Feedback-related GBRs were detected in five regions: (a) the pre-SMA of the frontal medial cortex [Brodmann's area (BA) 6 , superior frontal gyrus rostral to the VAC plane, defined as the vertical plane passing through the anterior commissure, with $0 < y < 20$ mm], (b) the dACC (BA 24/32/33), (c) the middle and inferior frontal gyrus exploring the DLPFC (BA 9/46), (d) the OFC (BA 11/12/13/14), and (e) in the anterior (ventral or dorsal) part of the insula.

The time course of the GBRs varied across the various anatomical structures. Figure 2 provides a summary of the time course of GBRs with respect to the presentation of feedback stimuli by pooling results from electrode sites belonging to the same anatomical cluster across all participants. Compared to positive feedback, negative feedback on performance triggered GBRs that were stronger in the pre-SMA, DLPFC, lateral OFC, and insula. The shortest latencies of activation were found in the DLPFC (peak of the response around 300 ms), followed by insula (peak latency around 500 ms), and lateral OFC (peak latency around 700 ms). In these three clusters, the duration of the responses lasted less than 1,000 ms. By contrast, the responses of the pre-SMA were sustained and lasted almost 2,000 ms. Positive feedback triggered GBRs in the medial OFC and dACC. In the medial OFC, the peak latency of the responses was around 500 ms and activation lasted less than 1,000 ms, while dACC activation was more gradual and sustained more than 1,000 ms. These findings provide an overview of the spatiotemporal properties of the positive versus negative feedback processing network. We will now describe the detected responses in more detail for each anatomical component of the network.

Pre-supplementary motor area

We observed GBRs to feedback stimuli in the pre-SMA of five patients (see Fig. 3). Those responses were found in spatially tightly confined regions ($7 < \text{abs}(x) < 11$; $2 < y < 10$; $50 < z < 54$ in Talairach space), in both right (four sites) and left (one site) hemispheres. On the individual MRI, all sites were located rostral to the VCA line and thus precisely in the pre-SMA (Picard and Strick, 1996). Although GBRs also occurred in response to positive feedback, the responses were significantly stronger for negative feedback ($P < 0.05$ for each site, Mann–Whitney U test). The time profile of the responses consisted of a sustained energy increase between 500 and 2,000 ms or more. The peak amplitude of GBRs in the pre-SMA was 13.0 ± 1 (SEM) for negative feedback and 9.1 (± 0.8) for positive feedback. The peak latency of GBRs in the pre-SMA was 860 ms for negative feedback and 840 ms for positive feedback.

Anterior cingulate cortex (BA 24/32/33)

Among electrodes present in dACC, two sites responded to feedback in the dACC (two patients, Fig. 3). Both were located in the dorsal portion of the anterior cingulate gyrus ($17 < y < 32$, Talaraich space) and had enhanced high-frequency responses to positive feedback ($P < 0.05$ for each site, Mann–Whitney U test), although negative feedback also triggered a high-frequency response. Both responses were gradual energy increases peaking around 800 ms and lasting 1,500 ms. The peak amplitude of GBRs in the dACC was 5.4 ± 0.7 for negative feedback and 11.7 ± 0.8 for positive feedback. The peak latency of GBRs in the dACC was 1,064 ms for negative feedback and 640 ms for positive feedback.

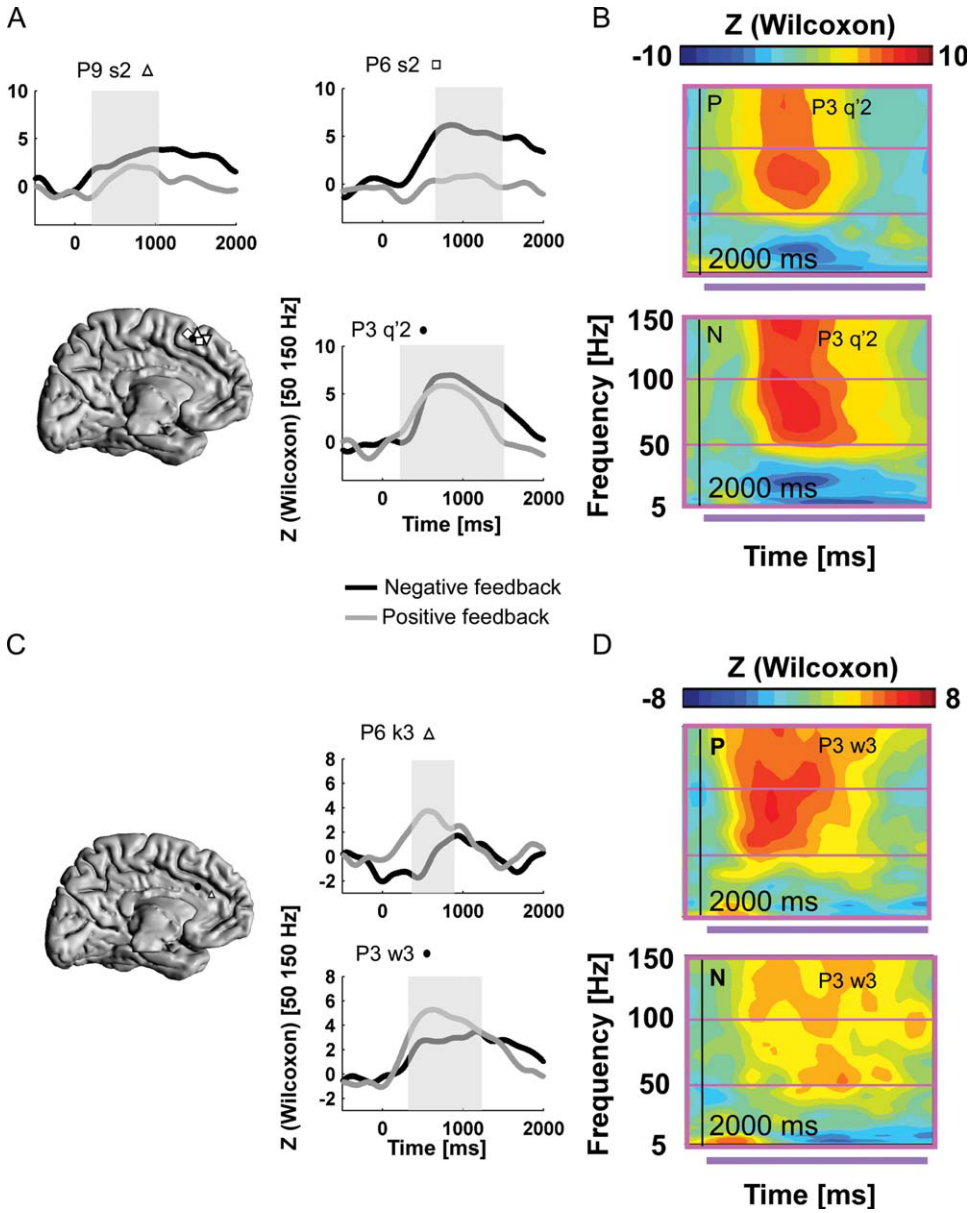

Figure 3.

GBRs in the medial frontal wall in the PM task. (**A**) and (**B**) show responses in the pre-SMA, while (**C**) and (**D**) show responses in the anterior cingulate gyrus (dACC). (A, C) The anatomical picture shows the locations of the corresponding sites reconstructed onto the MNI single-subject MRI. The time course of GBRs (50–150 Hz) for the two types of feedback is displayed, and segments with statistically significant differences between positive and negative feedback are shown as shaded regions. Three typical responses are shown for the pre-SMA (A) and two for the dACC (C). (B, D) Two representative examples of GBRs for one site in the pre-SMA (P3 q′2) and one site in the dACC (P3 w3) are shown on the right with TF maps for positive (upper map) and negative feedback (lower map). [Color figure can be viewed in the online issue, which is available at www.interscience.wiley.com.]

Middle frontal gyrus—DLPFC (BA 9/46)

As shown in Figure 4, responses to feedback were also found in the DLPFC (a total of four sites in four patients). GBRs were found both in response to positive feedback and negative feedback. Although one site in the right hemisphere had similar responses to both types of feedback (not shown in the Fig. 4), the three remaining sites, in the left hemisphere, had significantly stronger responses to negative feedback ($P < 0.05$, Mann–Whitney U test).

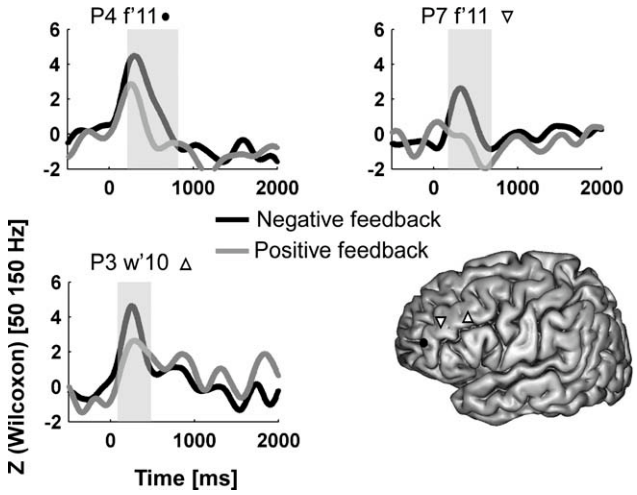

Figure 4.

GBRs in the DLPFC in the PM task. Anatomical locations of DLPFC sites are shown for three participants onto the MNI single-subject 3D MRI reconstruction. The time course of GBRs (50–150 Hz) for the two types of feedback is displayed, and segments with statistically significant differences between positive and negative feedback are shown as shaded regions.

The three left hemispheric responses were all characterized by a sudden short-lasting (less than 600 ms) energy increase in the first 300 ms following feedback presentation.

The peak amplitude of GBRs in the DLPFC was 11.0 ± 1.4 for negative feedback and 5 ± 1.5 for positive feedback. The peak latency of GBRs in the DLPFC was 281 ms for negative feedback and 281 ms for positive feedback.

Orbitofrontal cortex (BA 10/11/12/13/14)

Two anatomically and functionally distinct clusters in the OFC were found to generate feedback-specific γ-range activity (see Fig. 5). In a first, medial cluster (four sites), GBRs were stronger for positive feedback ($P < 0.05$, Mann–Whitney U test), while in a second, lateral cluster, responses were stronger for negative feedback (two sites). The two groups were well-separated anatomically: medial responses were all located in the medial OFC, more precisely in-between the lateral orbital sulcus and the gyrus rectus ($25 < \text{abs}(x) < 32$, Talairach space), while lateral sites were more lateral than the lateral orbital sulcus ($40 < \text{abs}(x) < 42$). In the medial OFC, the response was mostly a progressive energy increase within 400 ms and a gradual return to baseline after 1,000 ms (P1 k7, P3 e′8, P2 e7), although one site (P5 o6) had faster dynamics. Lateral OFC responses were shorter than 1,000 ms, with a sharp energy increase in the first 500 ms.

The peak amplitude of GBRs in the medial OFC was 6.5 ± 1.1 for negative feedback and 10.6 ± 0.9 for positive feedback. The peak latency of GBRs in the medial was 281 ms for negative feedback and 312 ms for positive feedback. The peak amplitude of GBRs in the lateral OFC was 13.3 ± 2.0 for negative feedback and 1.8 ± 1.0 for positive feedback. The peak latency of GBRs in the lateral OFC was 640 ms for negative feedback and 750 ms for positive feedback.

Insular γ-range activity during feedback processing

The remaining cluster was in the insula (see Fig. 6), where both types of feedback elicited γ-band energy increase in six sites (across four patients). In the anterior part of the insula (four sites), the response was fast, short, and stronger for negative feedback (within the first 1,000 ms with a peak around 500 ms). In the two remaining sites, located in the posterior part of insula for one site and in the ventral part of the insula for the other, the response was more gradual. One site in the ventral site had stronger response for positive feedback (P3 t′3). The peak amplitude of GBRs in the insula was 13.4 ± 0.7 for negative feedback and 7.9 ± 0.6 for positive feedback. The peak latency of GBRs in the insula was 437 ms for negative feedback and 359 ms for positive feedback.

γ Deactivations Induced by Feedback Stimuli in the PM Task

In addition to the poststimulus power increases reported above, we also observed that feedback induced power decreases in the same frequency range (high γ-band) along the medial frontal wall (12 sites in eight patients). γ-band energy suppressions were all located in the medial frontal cortex rostral to the pre-SMA or in the gyrus rectus (most medial part of the OFC) (see Fig. 7). Most suppression patterns (eight sites) were comparable for positive and negative feedback, but in four sites, the suppression occurred only in response to one type of feedback: either positive (two sites, P9 f2 and P9 w3) or negative (two sites, P2 f2 and P3 e′2). The time profile of deactivation was fairly reproducible across sites and participants and consisted of a sharp decrease of energy in the first 500 ms followed by a gradual return to baseline level within 1,000–1,500 ms.

Evoked Potentials and θ-Band Activity in the Anterior Cingulate in Response to Feedback Stimuli

Both negative and positive feedback generated ERPs in a large number of frontal sites. However, the ERPs were complex, with multiple positive and negative peaks, and extremely variable from site to site, and from patient to patient, even within the same region. We could not extract reproducible patterns and meaningful information from the ERPs. For this reason, we chose to keep the focus of this report on the robust and consistent GBRs rather than

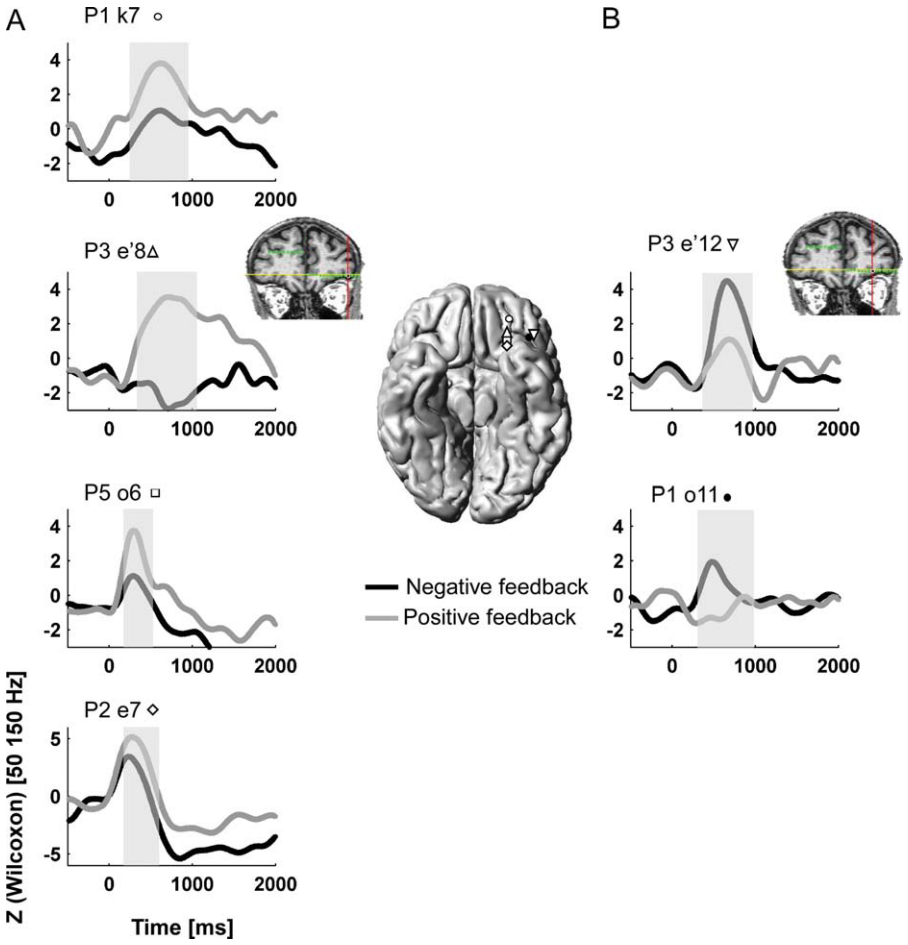

Figure 5.
GBRs in the OFC in the PM task. Anatomical locations of OFC sites are shown for six participants onto the standard MNI single-subject 3D MRI reconstruction. (**A**) For the four sites in the medial OFC, GBRs were stronger for positive feedback than negative feedback. The time course of GBRs (50–150 Hz) for the two types of feedback is displayed, and segments with statistically significant differences between positive and negative feedback are shown as shaded regions. (**B**) By contrast, for the two sites in the lateral OFC, GBRs were stronger for negative feedback than positive feedback. The time course of GBRs (50–150 Hz) for the two types of feedback is displayed, and segments with statistically significant differences between positive and negative feedback are shown as shaded regions. Note that for a particular patient, a stringent dissociation between lateral and medial OFC responses was found (medial P3 e′8 and lateral P3 e′12) and the anatomical locations of those two sites are displayed on the patient's MRI. [Color figure can be viewed in the online issue, which is available at www.interscience.wiley.com.]

to perform a detailed description of ERPs generated by the feedback stimuli. However, since noninvasive EEG studies in humans have consistently reported generators of a specific ERP, the FRN, in the anterior cingulate gyrus, we investigated ERPs specifically in that region. Out of 11 sites in the dorsal dACC, we found ERPs to feedback stimuli in six sites (see Fig. 8) around 300 ms, out of which four differed between types of feedback: a larger amplitude for negative feedback ($P < 0.05$, Kruskal–Wallis test) was found at those four sites at specific latency ranges (P3 k′2 between 620 and 940 ms, P3 w′3 between 400 and 640 ms, P8 i2 between 500 and 600 ms, and P9 z2 between 300 and 620 ms) ($P < 0.05$, Kruskal–Wallis test). Our ERP results are therefore consistent with the hypothesis that the dACC generates a response to negative feedback in a late-latency window after 300 ms. This late component, peaking later than the typical scalp latency of the FRN, might possibly constitute an intracranial correlate of the scalp P300 or Pe (Herrmann et al., 2004; Polich, 2007). We did not find any evidence of a specific response to negative feedback between 200 and 300 ms, that is in the latency range of the scalp FRN. Lastly, since recent work suggests that the FRN may be considered as a θ-band (4–7 Hz) oscillation (Luu et al., 2003), we looked for task-related θ-band activity modulations in the dACC. Out of 11 sites exploring the dACC, only two sites generated short-lasting (<600 ms) θ-band activity modulations in response to feedback stimuli (P3 w′3 and P6 k3). An example of feedback-induced θ-band activity modulation is shown in Supporting Information Figure 6. Note that those two sites also generated GBRs in response to feedback stimuli.

DISCUSSION

The present study is, to our knowledge, the first to assess the large-scale neural dynamics of PM using direct neural recordings of high γ-range neural activity in humans. By combining an unprecedented spatiotemporal resolution with single-trial TF analysis, the present study extends our knowledge about the neural substrates of feedback processing. First of all, we found that feedback stimuli activate a large-scale network of frontoinsular brain regions indexed by widely distributed high γ (>50 Hz) power modulations. This network includes the dorsal anterior cingulate gyrus (dACC) and the pre-SMA in the frontal medial cortex, the DLPFC, the OFC, and the anterior insula. This frontoinsular network responds to

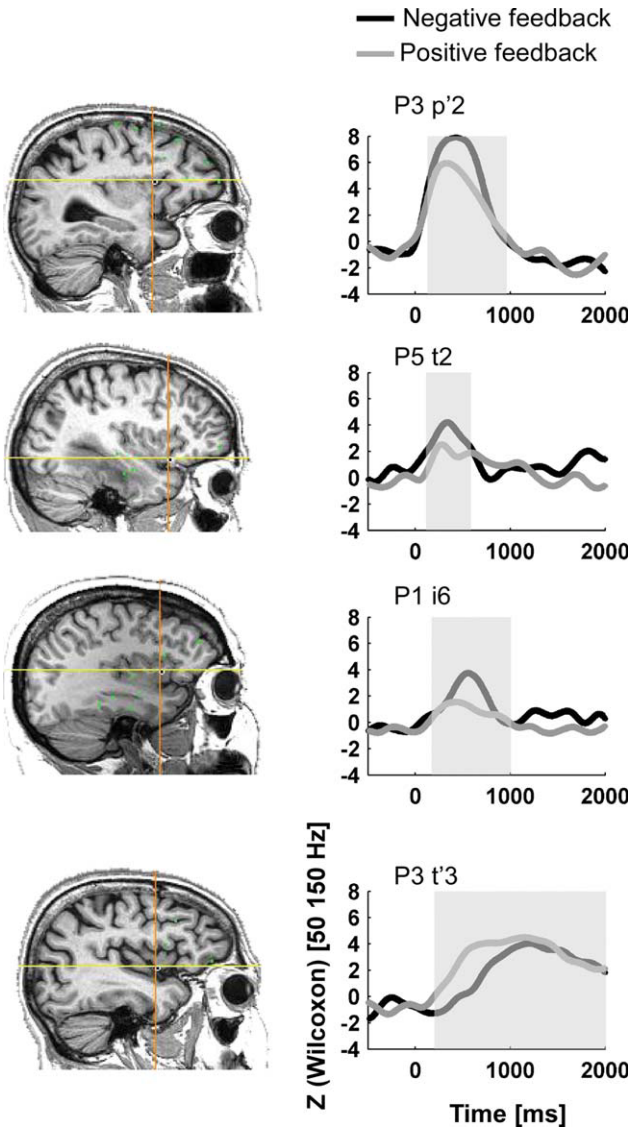

Figure 6.
GBRs in the insula in response to feedback on performance. In six sites across four patients, feedback stimuli induced GBRs. For five sites in the anterior insula (four sites) or posterior insula (one site), GBRs were stronger for negative feedback than positive feedback. For one site in the inferior insula, GBRs were stronger for positive feedback than for negative feedback. The anatomical pictures show the corresponding sites reconstructed onto individual subject MRIs for four of those sites generating typical GBRs. The time course of GBRs (50–150 Hz) for the two types of feedback is displayed, and segments with statistically significant differences between positive and negative feedback are shown as shaded regions. Four typical responses are shown for the anterior insula (three upper waveforms) and one for the inferior insula (bottom waveform). [Color figure can be viewed in the online issue, which is available at www.interscience.wiley.com.]

feedback with an increase of neural activity in the γ-band, referred to here as GBRs, while specific regions in the medial frontal cortex show a transient interruption of pre-stimulus γ-band activity. Moreover, we show that the time course of the activations in those regions is largely time-overlapping but distinct: the DLPFC, the insula, and the OFC displayed short responses lasting less 1,000 ms; on the contrary, responses in the pre-SMA and the dACC were more sustained and lasted more than 1,000 ms. Finally, we found that each component of this network is preferentially tuned to one type of feedback: the medial OFC and dACC respond stronger to positive feedback, while pre-SMA, DLPFC, lateral OFC, and anterior insula have stronger responses following negative feedback.

Before discussing this network, let us first consider possible interpretations for the high-frequency population-level activity found here. The current understanding of GBRs is that they correspond to a local synchronization mechanism that facilitates neural communication: increased γ-band activity would thus mean that neurons

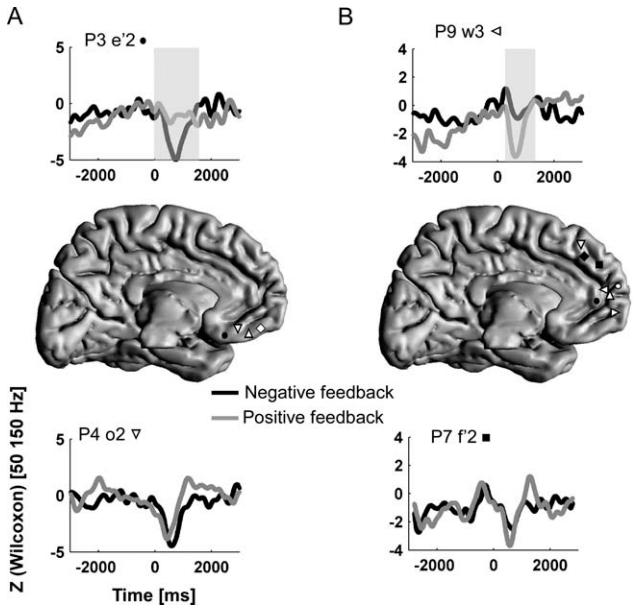

Figure 7.
γ-band suppressions in the gyrus rectus of the OFC (**A**) and in the medial prefrontal cortex (**B**) in the PM task. For four sites, feedback stimuli induced transient γ-band suppressions in the gyrus rectus (A) and for eight sites feedback stimuli induced transient γ-band suppressions in the medial prefrontal cortex (B). The anatomical locations of those sites are shown onto the standard MNI single-subject 3D MRI reconstruction for sites in the medial prefrontal cortex and gyrus rectus. Two typical time course of γ-band suppressions (50–150 Hz) in the gyrus rectus (A) and medial prefrontal cortex (B) for the two types of feedback are displayed, and segments with statistically significant differences between positive and negative feedback are shown as shaded regions.

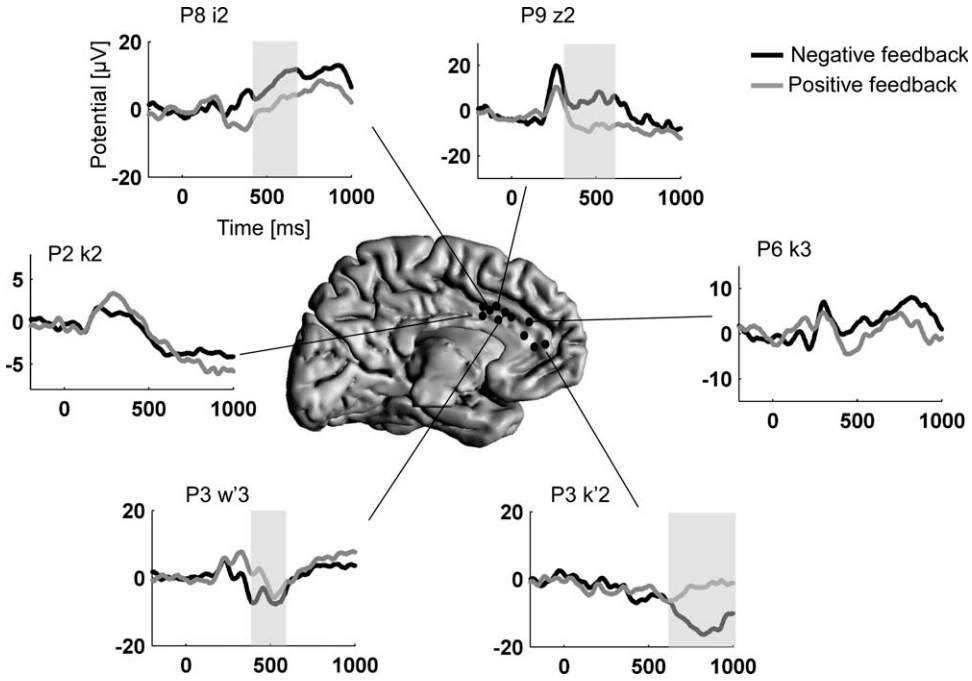

Figure 8.

ERPs in the dorsal anterior cingulate gyrus. The anatomical locations of six sites in dorsal anterior cingulate gyrus for which ERPs were found in response to feedback stimuli are shown onto the standard MNI single-subject 3D MRI reconstruction. ERPs for the two types of feedback are displayed, and segments with statistically significant differences between positive and negative feedback are shown as shaded regions. In three of the six sites, ERP amplitude was stronger for negative feedback (after 400 ms), while in one site, ERP amplitude was stronger for positive feedback (after 400 ms).

around the electrode get recruited by the task-at-hand (Jacobs et al., 2007; Nir et al., 2007). By analogy, γ-band suppressions, that is, transient decrease in γ-band energy, would correspond to an interruption of local communication and a withdrawing from the task (Lachaux et al., 2008). For this reason, GBRs have been proposed as precise markers of the cortical networks underlying cognition (Jensen et al., 2007; Jerbi et al., 2009; Lachaux et al., 2003), a suggestion that has meanwhile received further support by studies of multiple cognitive processes. Still, cognitive processes such as working memory or spatial navigation may also trigger activity modulations in other frequency bands, such as task-induced θ-band (4–7 Hz) modulations (Ekstrom et al., 2005; Raghavachari et al., 2001). The observation that both γ and θ power increases during cognitive processing may suggest that the two rhythms interact with each other. Indeed, θ–γ interactions have been reported in humans (Canolty et al., 2006).

Evaluating the Outcome of Actions Triggers Responses in Widespread Frontal Regions

Feedback induced GBRs in two distinct regions of the frontal medial wall, in the dorsal dACC (dACC) and the pre-SMA. The recruitment of dACC during feedback processing has been well-established, both in humans and monkeys; however, the exact nature of the dACC response is still under debate. EEG studies in humans have localized in the dACC the source of a FRN, between 200 and 300 ms after performance feedback (Miltner et al., 1997). The FRN has been observed in simple learning tasks and monetary gambling games and is larger in amplitude for negative feedback (Nieuwenhuis et al., 2004). Those results have been interpreted as evidence for a dACC-generated FRN specific to negative feedback [although that view has been recently challenged (Holroyd et al., 2008)]. Our high-frequency results contradict the view that the dACC would respond specifically to negative feedback, since GBRs were larger for positive feedback. This apparent discrepancy between noninvasive and invasive EEG results is most likely explained by the fact that the FRN and dACC GBRs correspond to different neural phenomena with distinct frequency ranges and possibly different functions. Indeed, ERP analysis of our data revealed consistent differences between feedback types after 300 ms in dACC sites, that is, at a slighty longer latency than the scalp FRN. This latency range is more compatible with the P300 or Pe recorded with scalp-EEG. Therefore, our results suggest that the dACC contributes possibly to the P300 or Pe

recorded with scalp-EEG, but not directly to the FRN (Herrmann and Knight, 2001; Herrmann et al., 2004; Polich, 2007).

Our observations are in line with recent studies in monkeys showing responses in the dACC to both correct and error feedback, even in single neurons (Michelet et al., 2007; Quilodran et al., 2008). These studies suggest that the stronger response we observed here to positive feedback, in two patients, might not be a general property of dACC neurons. On the whole, our findings indicate that the human dACC is not specifically and certainly not by itself involved solely in error detection. Our data fit better with the view that the dACC monitors the consequences of our own actions for online behavioral adaptation (Rushworth et al., 2004). In this view, both positive and negative feedback would activate the dACC, to reinforce or correct previous behavior.

Lastly, the dACC is also supposed to be the origin of θ-band (4–7 Hz) activity modulations in response to feedback stimuli. Our data indeed show transient (<400 ms) θ-band activity modulations in two patients. It is noteworthy that the two dACC sites generating GBRs also generated GBRs, in line with previous studies showing links between γ- and θ-band modulations (Canolty et al., 2006). Further work including more responding sites is needed to evaluate the possibility of cross-frequency coupling in those frequency bands.

Still, these short θ-band activity modulations do not provide any evidence that the underlying activity is rhythmic in the sense of repeating over multiple cycles. Power increase in the θ range could also result from the TF transformation of evoked potentials.

Not far from the dACC, feedback stimuli also activated the pre-SMA. However, pre-SMA sites had stronger responses to negative feedback, which is consistent with several fMRI findings (Ullsperger and von Cramon, 2003; Zanolie et al., 2008). The pre-SMA responses can be interpreted in multiple ways, since the pre-SMA has been associated with several cognitive systems mediating attention (Hon et al., 2006), motor planning (Akkal et al., 2002), and time estimation (Coull et al., 2004). In the present experiment, the task involved the production of a stereotyped motor pattern, defined by precise timing demands. The pre-SMA is known to be involved in planning sequences of movements, and for instance, pre-SMA neurons are recruited when monkeys update motor plans for subsequent temporally ordered movements (Shima et al., 1996). This suggests that in the present task, pre-SMA responses to feedback might participate in reshaping the precise motor pattern that has to be produced for successful task completion (Isoda and Hikosaka, 2007).

Feedback also elicited responses in the DLPFC, which were stronger for negative feedback. This effect has been seldom reported in humans [but see Zanolie et al. (2008)]. Neuroimaging studies have associated the DLPFC with related processes such as error monitoring (Debener et al., 2005) or rule switching (Monchi et al., 2001), but direct evidence of DLPFC activation during PM was lacking. In contrast, DLPFC responses to feedback have already been reported in monkeys: in animals learning arbitrary action-outcome contingencies, Matsumoto et al. (2007) have found neurons responding to feedback in the lateral PFC. However, cells did not differentiate positive and negative feedbacks. This led the authors to suggest that DLPFC neurons participate in directing attention toward the feedback stimulus. This interpretation does not conflict with our observation that negative feedback produced the strongest responses, because one might expect negative feedback to trigger a stronger attentional reaction than positive feedback for the given paradigm.

Lastly, robust responses to feedback were also observed in the OFC with a functional dissociation along a medial–lateral axis. Medial sites, between the gyrus rectus and lateral orbital sulcus, had stronger responses to positive feedback (Talairach coordinates: $25 < x < 32$). Sites more lateral than the lateral orbital sulcus had stronger responses to negative feedback ($x > 40$). Our results provide a direct confirmation that medial OFC is preferentially activated by rewarding stimuli and the lateral OFC by punishing stimuli (Kringelbach, 2005). This dissociation was exemplified in one participant (P3) with recordings from both medial and lateral parts of the OFC showing opposite responses (sites e′8 and e′12 shown in Fig. 5). More generally, our observations are in line with a large body of evidence, both in monkeys and humans, that the OFC is a key structure for estimating the reward value of external stimuli (Rolls, 2004) to guide behavior (Wallis, 2007).

Insular Responses During Feedback Processing

In complement to frontal activations, feedback stimuli produced strong responses in the anterior insula, at rather short latencies before 700 ms. The most likely interpretation is that this region participates in the emotional reaction to feedback. In this sense, our results would suggest that the reaction, in the context of the particular task used here, is stronger for negative feedback. The anterior agranular insula is part of a system underlying emotional processes. More specifically, it is involved in visceromotor, i.e. autonomic (Verberne and Owens, 1998) as well as in visceral sensory functions, underlying interoceptive awareness (Critchley, 2005), which is closely related to emotional reactions. Our interpretation is in line with a recent proposal that anterior insula might be involved in error awareness (Klein et al., 2007). As suggested by Klein et al. (2007), the response of the insula after negative feedback may be attributed to an enhanced awareness of the autonomic reaction to the error, or to the higher autonomic response itself, favoring error awareness.

Temporal Dynamics of the GBRs Within the Feedback-Processing Network

Little is known about the timing of neural responses in response to feedback in the human brain. The only information available so far has come from scalp EEG and MEG studies, which lack the sufficient spatial resolution to decipher the precise timing of individual brain regions. Our main result is that the timing of activation within the frontoinsular network is heterogeneous. This is a clear indication that feedback processing involves several distinct subprocesses that might be performed separately by the brain regions highlighted above. The main distinction is between "sustained" responses in the mesial frontal wall (dACC and pre-SMA) and more transient responses in the DLPFC, the OFC, and the insula. It is clear that the neural responses to feedback last way beyond 500 ms, that is beyond the FRN observed at the scalp level. Still, data from patients with electrodes recording from several clusters indicate possible sequence of activation within that network, more as a propagating wave than as a strict succession of responses. In this regard, data from patient P3 are particularly illustrative of a sequence starting in the DLPFC, and reaching in turn the insula, then the OFC, and finally the frontal medial wall. Although restricted to one patient, such timing observations are more in line with a succession of processes than with a global and integrated network processing feedback information as a whole through strong reciprocal interactions between simultaneous activations (Varela et al., 2001).

Transient Deactivations in the Medial Prefrontal Cortex During Feedback Processing

In sharp contrast with the activations just described, we observed in restricted parts of the medial frontal cortex a rare phenomenon referred to as negative GBRs, or γ-band suppressions (GBS). Those suppressions were characterized by a transient energy decrease in the γ-band after feedback stimuli. The phenomenon was observed in medial sites anterior to the pre-SMA and in most medial sites (gyrus rectus) of the OFC. The physiological meaning of GBS is not precisely known. The most obvious interpretation is that they correspond to local neural desynchronization and the interruption of local ongoing neural communication to attend specific demands of the cognitive task at hand. GBS have already been found during reading tasks in the ventral lateral prefrontal cortex (VLPFC) and were modulated by attention (Lachaux et al., 2008). Here, the spatial origin is different and, interestingly, it matches with a subportion of the so-called "default mode network." The default mode network is a common and reproducible network of brain areas less active during cognitive tasks than during rest, irrespective of the task (Raichle et al., 2001). This network has been identified with fMRI and PET and includes the ventromedial prefrontal cortex (V-MPFC), perhaps extending into the dACC, the posterior cingulate/precuneus/retrosplenial cortex, and the left and right lateral parietal cortices in the region of the angular gyri (Raichle and Snyder, 2007). Based on recent evidence that γ-band activity and BOLD signals appear to be stronlgy related (see above), we suggest that GBS corresponds to the deactivations found in neuroimaging studies. If this is the case, our observations would be the first direct evidence of reduced neural activity in the default network during a cognitive task. The temporal resolution of iEEG reveals that neural γ-range deactivations in the V-MPFC have a stereotyped time course, with a peak around 500 ms and a duration below 1,000 ms.

Several recent studies have implicated the anteromedial cortex in tasks requiring self-referencing and monitoring (Gusnard et al., 2001; Johnson et al., 2002). Accordingly, deactivation of this region has been interpreted as a temporary suppression of self-related activity during demanding tasks oriented toward external stimuli. In this view, deactivation of the V-MPFC indexed by GBS in our task would correspond to an attentional shift from the internal to the external world.

CONCLUSIONS

In summary, this study provides a detailed picture of the neural dynamics of the brain responses to success and failure in humans. Our results show that feedback on one's performance are processed by a large-scale network of distributed γ-range activations involving frontoinsular regions. We also demonstrate that, far from being functionally homogeneous, the dynamics of the network are differentially tuned: different regions of this network have distinct timing of activation and different sensitivity to the valence of feedback. Taken together, the results reported here provide novel insights into the intricate neural dynamics at play when our brain is faced with feedback on our performance. Finally, a better understanding of the central mechanism mediating feedback processing is bound to have direct implications on our knowledge of various cognitive processes such as adaptive behavior, skill acquisition, and ultimately of ways to improve them.

ACKNOWLEDGMENTS

We thank Pierre-Emmanuel Aguera and Patrick Bouchet for their valuable technical assistance and the Hospices Civils de Lyon.

REFERENCES

Akkal D, Bioulac B, Audin J, Burbaud P (2002): Comparison of neuronal activity in the rostral supplementary and cingulate motor areas during a task with cognitive and motor demands. Eur J Neurosci 15:887–904.

Alexander MP, Stuss DT, Picton T, Shallice T, Gillingham S (2007): Regional frontal injuries cause distinct impairments in cognitive control. Neurology 68:1515–1523.

Canolty RT, Edwards E, Dalal SS, Soltani M, Nagarajan SS, Kirsch HE, Berger MS, Barbaro NM, Knight RT (2006): High gamma power is phase-locked to theta oscillations in human neocortex. Science 313:1626–1628.

Cools R, Clark L, Owen AM, Robbins TW (2002): Defining the neural mechanisms of probabilistic reversal learning using event-related functional magnetic resonance imaging. J Neurosci 22:4563–4567.

Coull JT, Vidal F, Nazarian B, Macar F (2004): Functional anatomy of the attentional modulation of time estimation. Science 303:1506–1508.

Critchley HD (2005): Neural mechanisms of autonomic, affective, and cognitive integration. J Comp Neurol 493:154–166.

Debener S, Ullsperger M, Siegel M, Fiehler K, von Cramon DY, Engel AK (2005): Trial-by-trial coupling of concurrent electroencephalogram and functional magnetic resonance imaging identifies the dynamics of performance monitoring. J Neurosci 25:11730–11737.

Ekstrom AD, Caplan JB, Ho E, Shattuck K, Fried I, Kahana MJ (2005): Human hippocampal theta activity during virtual navigation. Hippocampus 15:881–889.

Engel AK, Fries P, Singer W (2001): Dynamic predictions: Oscillations and synchrony in top–down processing. Nat Rev Neurosci 2:704–716.

Fries P, Nikolic D, Singer W (2007): The gamma cycle. Trends Neurosci 30:309–316.

Gehring WJ, Willoughby AR (2002): The medial frontal cortex and the rapid processing of monetary gains and losses. Science 295:2279–2282.

Genovese CR, Lazar NA, Nichols T (2002): Thresholding of statistical maps in functional neuroimaging using the false discovery rate. Neuroimage 15:870–878.

Gusnard DA, Akbudak E, Shulman GL, Raichle ME (2001): Medial prefrontal cortex and self-referential mental activity: Relation to a default mode of brain function. Proc Natl Acad Sci USA 98:4259–4264.

Herrmann CS, Knight RT (2001): Mechanisms of human attention: Event-related potentials and oscillations. Neurosci Biobehav Rev 25:465–476.

Herrmann MJ, Rommler J, Ehlis AC, Heidrich A, Fallgatter AJ (2004): Source localization (LORETA) of the error-related-negativity (ERN/Ne) and positivity (Pe). Brain Res Cogn Brain Res 20:294–299.

Holroyd CB, Nieuwenhuis S, Yeung N, Nystrom L, Mars RB, Coles MG, Cohen JD (2004): Dorsal anterior cingulate cortex shows fMRI response to internal and external error signals. Nat Neurosci 7:497–498.

Holroyd CB, Pakzad-Vaezi KL, Krigolson OE (2008): The feedback correct-related positivity: Sensitivity of the event-related brain potential to unexpected positive feedback. Psychophysiology 45:688–697.

Hon N, Epstein RA, Owen AM, Duncan J (2006): Frontoparietal activity with minimal decision and control. J Neurosci 26:9805–9809.

Isnard J, Guenot M, Ostrowsky K, Sindou M, Mauguiere F (2000): The role of the insular cortex in temporal lobe epilepsy. Ann Neurol 48:614–623.

Isoda M, Hikosaka O (2007): Switching from automatic to controlled action by monkey medial frontal cortex. Nat Neurosci 10:240–248.

Ito S, Stuphorn V, Brown JW, Schall JD (2003): Performance monitoring by the anterior cingulate cortex during saccade countermanding. Science 302:120–122.

Jacobs J, Kahana MJ, Ekstrom AD, Fried I (2007): Brain oscillations control timing of single-neuron activity in humans. J Neurosci 27:3839–3844.

Jensen O, Kaiser J, Lachaux JP (2007): Human gamma-frequency oscillations associated with attention and memory. Trends Neurosci 30:317–324.

Jerbi K, Ossandon T, Hamame C, Senova S, Dalal S, Jung J, Minotti L, Bertrand O, Berthoz A, Kahane P, Lachaux JP (2009): Task-related gamma-band dynamics from an intracerebral perspective: Review and implications for surface EEG and MEG. Hum Brain Mapp 30:1758–1771.

Johnson SC, Baxter LC, Wilder LS, Pipe JG, Heiserman JE, Prigatano GP (2002): Neural correlates of self-reflection. Brain 125(Pt 8):1808–1814.

Jung J, Hudry J, Ryvlin P, Royet JP, Bertrand O, Lachaux JP (2006): Functional significance of olfactory-induced oscillations in the human amygdala. Cereb Cortex 16:1–8.

Jung J, Mainy N, Kahane P, Minotti L, Hoffmann D, Bertrand O, Lachaux JP (2008): The neural bases of attentive reading. Hum Brain Mapp 29:1193–1206.

Kahana MJ (2006): The cognitive correlates of human brain oscillations. J Neurosci 26:1669–1672.

Klein TA, Endrass T, Kathmann N, Neumann J, von Cramon DY, Ullsperger M (2007): Neural correlates of error awareness. Neuroimage 34:1774–1781.

Kringelbach ML (2005): The human orbitofrontal cortex: Linking reward to hedonic experience. Nat Rev Neurosci 6:691–702.

Lachaux JP, Rudrauf D, Kahane P (2003): Intracranial EEG and human brain mapping. J Physiol Paris 97(4–6):613–628.

Lachaux JP, Fonlupt P, Kahane P, Minotti L, Hoffmann D, Bertrand O, Baciu M (2007): Relationship between task-related gamma oscillations and BOLD signal: New insights from combined fMRI and intracranial EEG. Hum Brain Mapp 28:1368–1375.

Lachaux JP, Jung J, Mainy N, Dreher JC, Bertrand O, Baciu M, Minotti L, Hoffmann D, Kahane P (2008): Silence is golden: Transient neural deactivation in the prefrontal cortex during attentive reading. Cereb Cortex 18:443–450.

Lee D (2003): Coherent oscillations in neuronal activity of the supplementary motor area during a visuomotor task. J Neurosci 23:6798–6809.

Logothetis NK, Pauls J, Augath M, Trinath T, Oeltermann A (2001): Neurophysiological investigation of the basis of the fMRI signal. Nature 412:150–157.

Luu P, Tucker DM, Derryberry D, Reed M, Poulsen C (2003): Electrophysiological responses to errors and feedback in the process of action regulation. Psychol Sci 14:47–53.

Mainy N, Kahane P, Minotti L, Hoffmann D, Bertrand O, Lachaux JP (2007): Neural correlates of consolidation in working memory. Hum Brain Mapp 28:183–193.

Mainy N, Jung J, Baciu M, Kahane P, Schoendorff B, Minotti L, Hoffmann D, Bertrand O, Lachaux JP (2008): Cortical dynamics of word recognition. Hum Brain Mapp 29:1215–1230.

Matsumoto M, Matsumoto K, Abe H, Tanaka K (2007): Medial prefrontal cell activity signaling prediction errors of action values. Nat Neurosci 10:647–656.

Michelet T, Bioulac B, Guehl D, Escola L, Burbaud P (2007): Impact of commitment on performance evaluation in the rostral cingulate motor area. J Neurosci 27:7482–7489.

Miltner WHR, Braun CH, Coles MGH (1997): Event-related brain potentials following incorrect feedback in a time-estimation task: Evidence for a 'generic' neural system for error detection. J Cogn Neurosci 9:788–798.

Monchi O, Petrides M, Petre V, Worsley K, Dagher A (2001): Wisconsin Card Sorting revisited: Distinct neural circuits participating in different stages of the task identified by event-related functional magnetic resonance imaging. J Neurosci 21:7733–7741.

Mukamel R, Gelbard H, Arieli A, Hasson U, Fried I, Malach R (2005): Coupling between neuronal firing, field potentials, and FMRI in human auditory cortex. Science 309:951–954.

Nieuwenhuis S, Holroyd CB, Mol N, Coles MG (2004): Reinforcement-related brain potentials from medial frontal cortex: Origins and functional significance. Neurosci Biobehav Rev 28:441–448.

Nieuwenhuis S, Slagter HA, von Geusau NJ, Heslenfeld DJ, Holroyd CB (2005): Knowing good from bad: Differential activation of human cortical areas by positive and negative outcomes. Eur J Neurosci 21:3161–3168.

Nir Y, Fisch L, Mukamel R, Gelbard-Sagiv H, Arieli A, Fried I, Malach R (2007): Coupling between neuronal firing rate, gamma LFP, and BOLD fMRI is related to interneuronal correlations. Curr Biol 17:1275–1285.

Picard N, Strick PL (1996): Motor areas of the medial wall: A review of their location and functional activation. Cereb Cortex 6:342–353.

Polich J (2007): Updating P300: An integrative theory of P3a and P3b. Clin Neurophysiol 118:2128–2148.

Polli FE, Barton JJ, Thakkar KN, Greve DN, Goff DC, Rauch SL, Manoach DS (2008): Reduced error-related activation in two anterior cingulate circuits is related to impaired performance in schizophrenia. Brain 131(Pt 4):971–986.

Quilodran R, Rothe M, Procyk E (2008): Behavioral shifts and action valuation in the anterior cingulate cortex. Neuron 57:314–325.

Raghavachari S, Kahana MJ, Rizzuto DS, Caplan JB, Kirschen MP, Bourgeois B, Madsen JR, Lisman JE (2001): Gating of human theta oscillations by a working memory task. J Neurosci 21:3175–3183.

Raichle ME, Snyder AZ (2007): A default mode of brain function: A brief history of an evolving idea. Neuroimage 37:1083–1090; discussion 1097–1099.

Raichle ME, MacLeod AM, Snyder AZ, Powers WJ, Gusnard DA, Shulman GL (2001): A default mode of brain function. Proc Natl Acad Sci USA 98:676–682.

Rolls ET (2004): The functions of the orbitofrontal cortex. Brain Cogn 55:11–29.

Ruchsow M, Grothe J, Spitzer M, Kiefer M (2002): Human anterior cingulate cortex is activated by negative feedback: Evidence from event-related potentials in a guessing task. Neurosci Lett 325:203–206.

Rushworth MF, Walton ME, Kennerley SW, Bannerman DM (2004): Action sets and decisions in the medial frontal cortex. Trends Cogn Sci 8:410–417.

Shima K, Mushiake H, Saito N, Tanji J (1996): Role for cells in the presupplementary motor area in updating motor plans. Proc Natl Acad Sci USA 93:8694–8698.

Singer W (1999): Neuronal synchrony: A versatile code for the definition of relations? Neuron 24:49–65, 111–125.

Talairach J, Tournoux P (1988): Co-planar Stereotaxic Atlas of the Human Brain. 3-Dimensional Proportional System: An Approach to Cerebral Imaging. Stuttgart: Thieme.

Tallon-Baudry C, Bertrand O, Delpuech C, Pernier J (1997): Oscillatory gamma-band (30–70 Hz) activity induced by a visual search task in humans. J Neurosci 17:722–734.

Thakkar KN, Polli FE, Joseph RM, Tuch DS, Hadjikhani N, Barton JJ, Manoach DS. (2008): Response monitoring, repetitive behaviour and anterior cingulate abnormalities in autism spectrum disorders (ASD). Brain 131(Pt 9):2464–2478.

Ullsperger M, von Cramon DY (2003): Error monitoring using external feedback: Specific roles of the habenular complex, the reward system, and the cingulate motor area revealed by functional magnetic resonance imaging. J Neurosci 23:4308–4314.

van Veen V, Holroyd CB, Cohen JD, Stenger VA, Carter CS (2004): Errors without conflict: Implications for performance monitoring theories of anterior cingulate cortex. Brain Cogn 56:267–276.

Varela F, Lachaux JP, Rodriguez E, Martinerie J (2001): The brainweb: Phase synchronization and large-scale integration. Nat Rev Neurosci 2:229–239.

Verberne AJ, Owens NC (1998): Cortical modulation of the cardiovascular system. Prog Neurobiol 54:149–168.

Wallis JD (2007): Orbitofrontal cortex and its contribution to decision-making. Annu Rev Neurosci 30:31–56.

Walton ME, Devlin JT, Rushworth MF (2004): Interactions between decision making and performance monitoring within prefrontal cortex. Nat Neurosci 7:1259–1265.

Zanolie K, Van Leijenhorst L, Rombouts SA, Crone EA (2008): Separable neural mechanisms contribute to feedback processing in a rule-learning task. Neuropsychologia 46:117–126.